

# EARTHS IN OTHER SOLAR SYSTEMS AND ALIEN EARTHS

## Recent Publications

*Bioverse: a simulation framework to assess the statistical power of future biosignature surveys*  
.....

*An Integrated Analysis with Predictions on the Architecture of the  $\tau$  Ceti Planetary System, Including a Habitable Zone Planet*  
.....

*Exoplanets are still out there - a new model tells astronomers where to look for more using 4 simple variables*  
.....

*Direct Imaging Discovery of a Young Brown Dwarf Companion to an A2V Star*  
.....

*Hints for icy pebble migration feeding an oxygen-rich chemistry in the inner planet-forming region of disks*  
.....

*The Evolution of Disk Winds from a Combined Study of Optical and Infrared Forbidden Lines*  
.....

*Carbon Isotope Ratios in Planetary Nebulae: The Unexpected Enhancement of  $^{13}\text{C}$*   
.....



**Earths in Other Solar Systems** and Alien Earths are part of NASA’s Nexus for Exoplanetary System Science program, which carries out coordinated research toward the goal of searching for and determining the frequency of habitable extrasolar planets with atmospheric biosignatures in the Solar neighborhood.

Our interdisciplinary teams includes astrophysicists, planetary scientists, cosmochemists, material scientists, chemists, biologists, and physicists.

The Principal Investigator of Project EOS and Alien Earths is Daniel Apai (University of Arizona). The projects’ lead institutions are The University of Arizona’s Steward Observatory and Lunar and Planetary Laboratory.

For a complete list of publications, please visit the [EOS Library](#) on the SAO/NASA Astrophysics Data System.

# EARTHS IN OTHER SOLAR SYSTEMS

# AND ALIEN EARTHS

## Recent Publications (cont.)

*ELT Imaging of MWC 297  
from the 23 m LBTI:*

*Complex Disk Structure and  
a Companion Candidate*

.....

*High-Resolution Mid-Infrared  
Spectroscopy of GV Tau N:  
Surface Accretion and  
Detection of Ammonia in a  
Young Protoplanetary Disk*

.....

*An Improved HR Diagram for  
the Orion Trapezium Cluster*

.....

*Proplyds in the flame nebula  
NGC 2024*

.....

*The First Extensive  
Spectroscopic Study of  
Young Stars in the North  
America and Pelican  
Nebulae*

.....

*A Disk-driven Resonance as  
the Origin of High  
Inclinations of Close-in  
Planets*

.....

*Observational Completion  
Limit of Minor Planets from  
the Asteroid Belt to Jupiter  
Trojans*

## Origins Seminar

The **Origins Seminar** series brings together ISM, star and planet formation people, exoplanets experts, planetary scientists and astrobiologists. Topics range from molecular clouds through star and planet formation to exoplanets detection and characterization and astrobiology.

The seminar series is organized by Serena Kim (SO), Kamber Schwarz (LPL), Sebastiaan Krijt (University of Exeter, UK) and Sebastiaan Haffert (SO) from Steward Observatory/Dept. of Astronomy and Dept. of Planetary Sciences (LPL) at the University of Arizona. The Origins Seminar series is partly supported by the Earths in Other Solar Systems NExSS team.

Talks take place **12:00 - 1:00pm (MST) on Mondays**. To receive weekly updates and advertisements for talks, please subscribe to the [mailing list](#). If you are interested in presenting your work during one of the open slots, feel free to contact [the organizers](#).

**Currently, the Origins seminar meets via Zoom due to the Covid-19 Pandemic.** We may continue to meet via zoom through Summer 2021, depending on the status of the Pandemic and guidelines by the department and the University. The Zoom information is sent via email.

[Origins Seminars YouTube Channel](#)

# Bioverse: a simulation framework to assess the statistical power of future biosignature surveys

Alex Bixel and Dániel Apai

→ [Accepted for publication in The Astronomical Journal](#)

Next-generation space observatories will conduct the first systematic surveys of terrestrial exoplanet atmospheres and search for evidence of life beyond Earth. While in-depth observations of the nearest habitable worlds may yield enticing results, there are fundamental questions about planetary habitability and evolution which can only be answered through population-level studies of dozens to hundreds of terrestrial planets. To determine the requirements for next-generation observatories to address these questions, we have developed Bioverse. Bioverse combines existing knowledge of exoplanet statistics with

a survey simulation and hypothesis testing framework to determine whether proposed space-based direct imaging and transit spectroscopy surveys will be capable of detecting various hypothetical statistical relationships between the properties of terrestrial exoplanets. Following a description of the code, we apply Bioverse to determine whether an ambitious direct imaging or transit survey would be able to determine the extent of the circumstellar habitable zone and study the evolution of Earth-like planets. Given recent evidence that Earth-sized habitable zone planets are likely much rarer than previously believed (Pascucci et al. 2019), we find that space missions with large search volumes will be necessary to study the population of terrestrial and habitable worlds. Moving forward, Bioverse provides a methodology for performing trade studies of future observatory concepts to maximize their ability to address population-level questions, including and beyond the specific examples explored here.

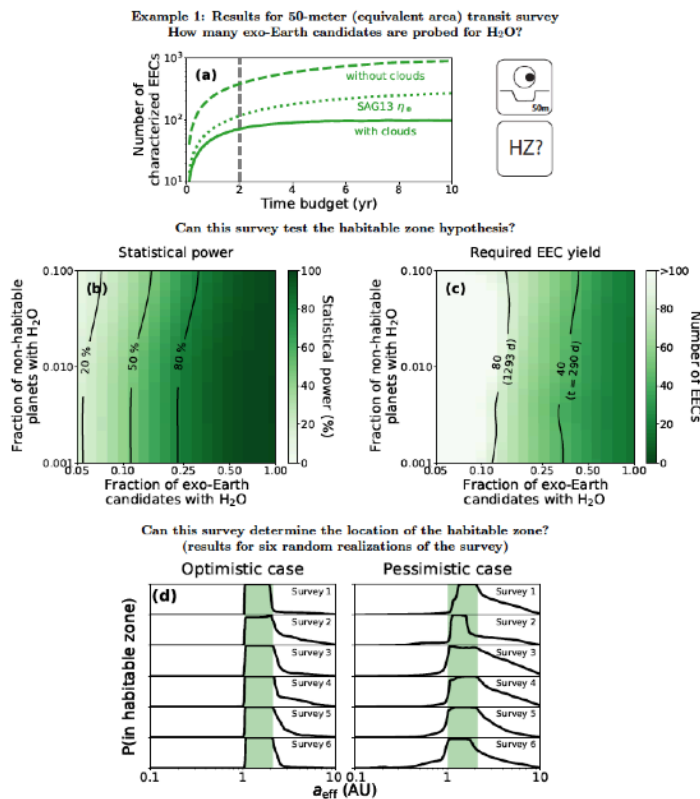


**Figure 7.** Results for the transit survey in Section 6. (a) The number of EECs observed versus the observing time budget, assuming  $\eta_{\oplus} = 7.5\%$  for G stars and cloudy atmospheres (solid). 4-10x as many planets could be observed if clouds were neglected (dashed), or 1.5-3x as many with clouds if assuming the higher SAG13 estimate of  $\eta_{\oplus} = 24\%$  (dotted). As our baseline case, we set  $t_{\text{total}} = 2$  yr. (b) The statistical power to test the habitable zone hypothesis as a function of the astrophysical parameters in Equation 13. (c) The minimum number of EECs which must be characterized to achieve 80% statistical power, with the necessary observing time budget  $t_{\text{total}}$ . (d) The posterior probability that a planet with effective separation  $a_{\text{eff}}$  is in the habitable zone, as estimated by six random realizations of the survey under an optimistic case (80% of EECs are habitable, left) and pessimistic case (20% of EECs are habitable, right). The true habitable zone is highlighted in green, and in both cases 1% of non-habitable planets have H<sub>2</sub>O.

## An Integrated Analysis with Predictions on the Architecture of the $\tau$ Ceti Planetary System, Including a Habitable Zone Planet

Jeremy Dietrich and Dániel Apai

→ [The Astronomical Journal, Volume 161, Number 1](#)

$\tau$  Ceti is the closest single Sun-like star to the solar system and hosts a multiplanet system with four confirmed planets. The possible presence of additional planets, especially potentially habitable worlds, remains of great interest. We analyze the structure of the  $\tau$  Ceti planetary system via the DYNAMITE algorithm, combining information from exoplanet population statistics and orbital dynamics with measurements of this specific system. We also expand DYNAMITE to incorporate radial velocity information. Our analysis suggests the presence of four additional planets, three of which match closely with the periods of three tentative planet candidates reported previously. We also predict at least one more planet candidate with an orbital period between  $\sim 270$  and  $470$  days, in the habitable zone for  $\tau$  Ceti. Based on the measured  $m \sin i$  values of the confirmed planets, we also assess the possible masses and nature of the detected and undetected planets. The least massive planets and candidates are likely to be rocky, while the other planets and

candidates could either be rocky or contain a significant gaseous envelope. The radial velocity observable signature from the predicted habitable zone planet candidate would likely be at or just above the noise level in current data, but should be detectable in future extremely high-precision radial velocity and direct-imaging studies.

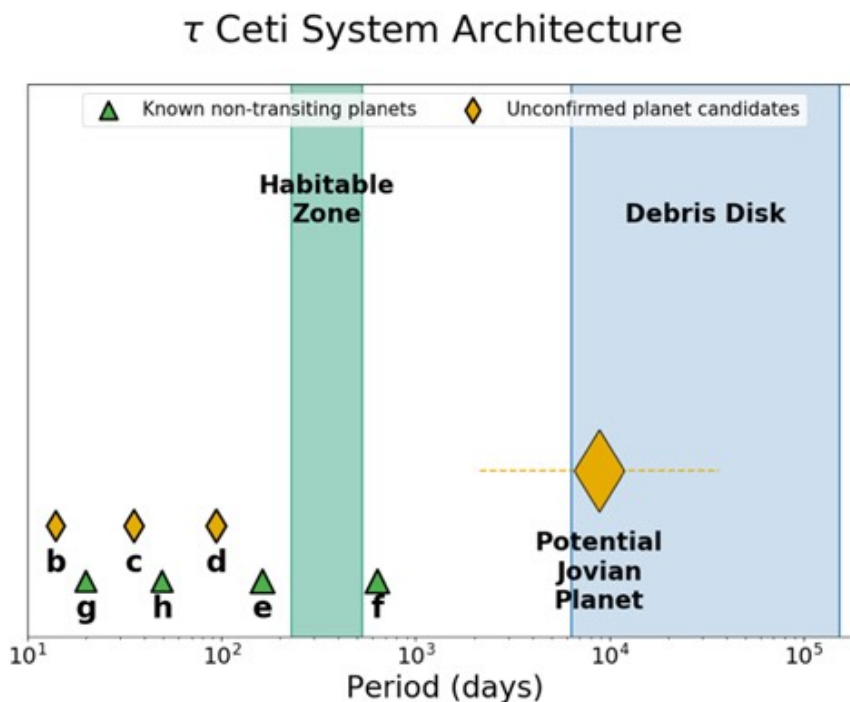


**Figure 1.** The  $\tau$  Ceti system architecture, with known planets, unconfirmed planet candidates (with large error bars for the tentative Jovian planet detection), and the extents of the habitable zone and the debris disk. Relative marker sizes match planet sizes.

## *Exoplanets are still out there - a new model tells astronomers where to look for more using 4 simple variables*

Dániel Apai and Jeremy Dietrich

---

### → [The Conversation, November 9, 2020](#)

Only 12 light years from Earth, Tau Ceti is the closest single star similar to the Sun and an all-time favorite in sci-fi stories. Habitable worlds orbiting Tau Ceti were destinations of fictional starships like "The Expanse"'s Nauvoo and "Barbarella"'s vessel. "Star Trek"'s Captain Picard also frequented an exotic bar in the system. Now, thanks to a new approach to analyzing nearby planetary systems, we have a deeper understanding of the actual worlds that orbit Tau Ceti and many other nearby stars.

Exoplanets - worlds around other stars - have long been staples of science fiction but remained mostly inaccessible to scientific investigations. This all changed over the past decade, when NASA's Kepler and TESS exoplanet hunter space telescopes added thousands of new planets to the previously short tally of alien worlds.

We have now developed a novel way to figure out whether there are yet-undiscovered planets in these systems.



Planetary orbits and habitable zone in the tau Ceti system, as derived from the analysis presented in Dietrich & Apai 2021.

## Direct Imaging Discovery of a Young Brown Dwarf Companion to an A2V Star

Kevin Wagner, Dániel Apai, Markus Kasper, Melissa McClure, Massimo Robberto, and Thayne Currie

### → [The Astronomical Journal Letters, Volume 902, Number 1](#)

We present the discovery and spectroscopy of HIP 75056Ab, a companion directly imaged at a very small separation of  $0''.125$  to an A2V star in the Scorpius-Centaurus OB2 association. Our observations utilized Very Large Telescope/Spectro-Polarimetric High-contrast Exoplanet Research Experiment between 2015 and 2019, enabling low-resolution spectroscopy ( $0.95\text{--}1.65\ \mu\text{m}$ ), dual-band imaging ( $2.1\text{--}2.25\ \mu\text{m}$ ), and relative astrometry over a four-year baseline. HIP 75056Ab is consistent with spectral types in the range of M6–L2 and  $T_{\text{eff}} \sim 2000\text{--}2600\ \text{K}$ . A comparison of the companion's brightness to evolutionary tracks suggests a mass of  $\sim 20\text{--}30\ M_{\text{Jup}}$ . The astrometric measurements are consistent with an orbital semimajor axis of  $\sim 15\text{--}45\ \text{au}$  and an inclination close to face-on ( $i \lesssim 35^\circ$ ). In this range of mass and orbital separation, HIP 75056Ab is likely at the low-mass end of the distribution of companions formed via disk instability, although a formation of the companion via core accretion cannot be excluded. The orbital constraints are consistent with the modest eccentricity values predicted by disk instability, a scenario that can be confirmed by further astrometric monitoring. HIP 75056Ab may be utilized as a low-mass atmospheric comparison to older, higher-mass brown dwarfs, and also to young giant planets. Finally, the detection of HIP 75056Ab at  $0''.125$  represents a milestone in detecting low-mass companions at separations corresponding to the habitable zones of nearby Sun-like stars.

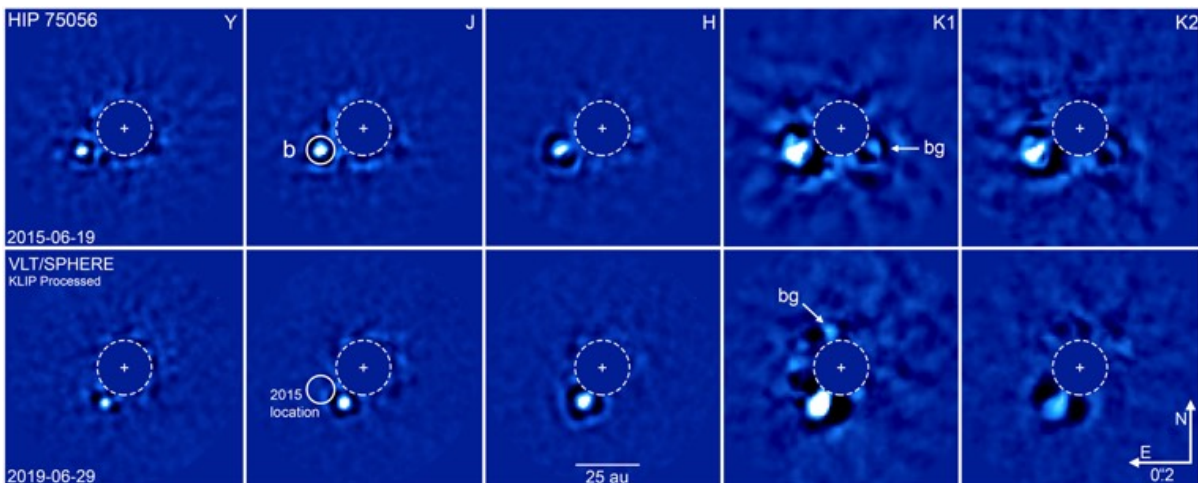


**Figure 1.** SPHERE images of HIP 75056Ab from 2015 (top row) and 2019 (bottom row) processed with KLIP. The source is clearly detected at each end of the ( $1\text{--}2.25\ \mu\text{m}$ ) bandpass at a separation of  $\sim 0''.155$  ( $0''.125$  in 2019). The object's motion with respect to HIP 75056A is consistent with orbital motion for a semimajor axis of  $a \sim 15\text{--}45\ \text{au}$  and is inconsistent with the expected motion of a background star. In the K1-band images, the relative positional change of the object labeled "bg" illustrates the proper motion of HIP 75056.

## Hints for icy pebble migration feeding an oxygen-rich chemistry in the inner planet-forming region of disks

Banzatti, Andrea; Pascucci, Ilaria; Bosman, Arthur D.; Pinilla, Paola; Salyk, Colette; Herczeg, Greg J.; Pontoppidan, Klaus M.; Vazquez, Ivan; Watkins, Andrew; Krijt, Sebastiaan; Hendl, Nathan; Long, Feng

### → [The Astrophysical Journal, Volume 903, Number 2](#)

We present a synergic study of protoplanetary disks to investigate links between inner disk gas molecules and the large-scale migration of solid pebbles. The sample includes 63 disks where two types of measurements are available: i) spatially-resolved disk images revealing the radial distribution of disk pebbles (mm-cm dust grains), from millimeter observations with ALMA or the SMA, and ii) infrared molecular emission spectra as observed with Spitzer. The line flux ratios of H<sub>2</sub>O with HCN, C<sub>2</sub>H<sub>2</sub>, and CO<sub>2</sub> all anti-correlate with the dust disk radius  $R_{dust}$ , expanding previous results found by Najita et al. (2013) for HCN/H<sub>2</sub>O and the dust disk mass. By normalization with the dependence on accretion luminosity common to all molecules, only the H<sub>2</sub>O luminosity maintains a detectable anti-correlation with disk radius, suggesting that the strongest underlying relation is between H<sub>2</sub>O and  $R_{dust}$ . If  $R_{dust}$  is set by large-scale pebble drift, and if molecular luminosities trace the elemental budgets of inner disk warm gas, these results can be naturally explained with scenarios where the inner disk chemistry is fed by sublimation of oxygen-rich icy pebbles migrating inward from the outer disk. Anti-correlations are also detected between all molecular luminosities and the infrared index  $n_{13-30}$ , which is sensitive to the presence and size of an inner disk dust cavity. Overall, these relations suggest a physical interconnection between dust and gas evolution both locally and across disk scales. We discuss fundamental predictions to test this interpretation and study the interplay between pebble drift, inner disk depletion, and the chemistry of planet-forming material.

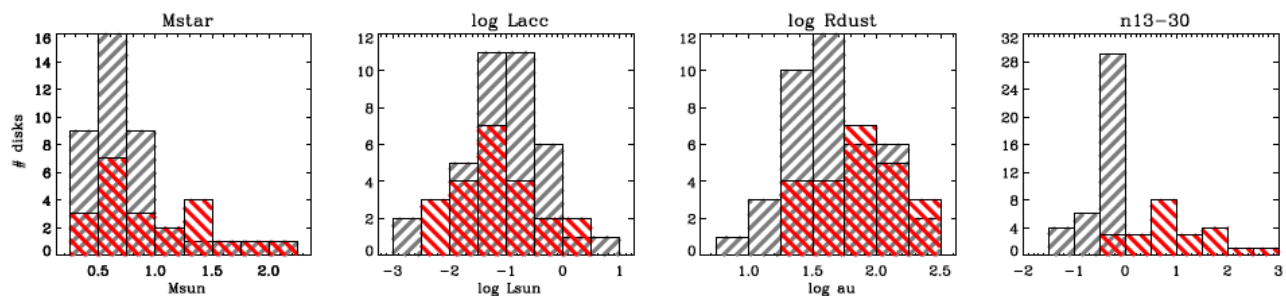


**Figure 1.** Sample property distributions (see Section 2 for details). Full disks are shown in grey; disks with inner cavities are shown in red.

## The Evolution of Disk Winds from a Combined Study of Optical and Infrared Forbidden Lines

Pascucci, I.; Banzatti, A.; Gorti, U.; Fang, M.; Pontoppidan, K.; Alexander, R.; Ballabio, G.; Edwards, S.; Salyk, C.; Sacco, G.; Flaccomio, E.; Blake, G. A.; Carmona, A.; Hall, C.; Kamp, I.; Kaufl, H. U.; Meeus, G.; Meyer, M.; Pauly, T.; Steendam, S. Sterzik, M.

### → [The Astrophysical Journal, Volume 903, Number 2](#)

We analyze high-resolution ( $dv < 10 \text{ km/s}$ ) optical and infrared spectra covering the [OI] 6300 angstrom and [NeII] 12.81 micron lines from a sample of 31 disks in different evolutionary stages. Following work at optical wavelengths, we use Gaussian profiles to fit the [NeII] lines and classify them into HVC (LVC) if the line centroid is more (less) blueshifted than 30 km/s with respect to the stellar radial velocity. Unlike for the [OI] where a HVC is often accompanied by a LVC, all 17 sources with a [NeII] detection have either a HVC or a LVC. [NeII] HVCs are preferentially detected toward high accretors ( $M_{\text{acc}} > 10^{-8} M_{\text{sun/yr}}$ ) while LVCs are found in sources with low  $M_{\text{acc}}$ , low [OI] luminosity, and large infrared spectral index ( $n_{13-31}$ ). Interestingly, the [NeII] and [OI] LVC luminosities display an opposite behaviour with  $n_{13-31}$ : as the inner dust disk depletes (higher  $n_{13-31}$ ) the [NeII] luminosity increases while the [OI] weakens. The [NeII] and [OI] HVC profiles are generally similar with centroids and FWHMs showing the expected behaviour from shocked gas in micro-jets. In contrast, the [NeII] LVC profiles are typically more blueshifted and narrower than the [OI] profiles. The FWHM and centroid vs. disk inclination suggest that the [NeII] LVC predominantly traces unbound gas from a slow, wide-angle wind that has not lost completely the Keplerian signature from its launching region. We sketch an evolutionary scenario that could explain the combined [OI] and [NeII] results and includes screening of hard ( $\sim 1 \text{ keV}$ ) X-rays in inner, mostly molecular, MHD winds.

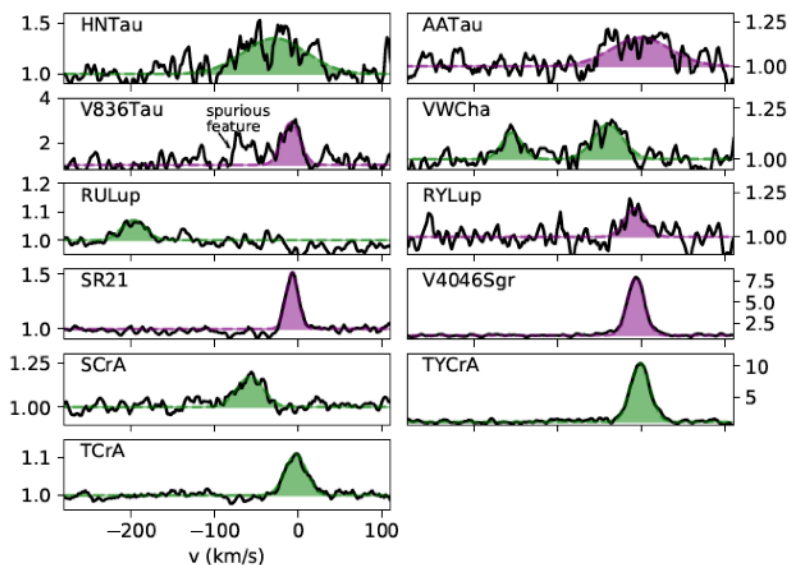


**Figure 1.** VISIR 2 spectra with a [Ne II] 12.8  $\mu\text{m}$  detection. For visualization purposes, we applied a boxcar smoothing of 3 velocity elements. For S CrA we show the spectrum from the fainter B component, see Figure 2 for the other component. The best fit Gaussian profiles are colored in green for the HVC and purple for the LVC following the assignments in Table 2.

# Carbon Isotope Ratios in Planetary Nebulae: The Unexpected Enhancement of $^{13}\text{C}$

L. M. Ziurys, D. R. Schmidt, and N. J. Woolf

➔ [The Astrophysical Journal Letters, Volume 900, Number 2](#)

The  $^{12}\text{C}/^{13}\text{C}$  ratio has been measured toward a sample of planetary nebulae (PNe) using millimeter observations of CO, HCN, HNC, CN, and other species, conducted with the 12 m antenna and the Submillimeter Telescope of the Arizona Radio Observatory. The observed nebulae spanned the entire lifetime of PNe, from  $\sim 900$  to 12,000 yr, and include well-known objects such as NGC 7293 (Helix), NGC 6720 (Ring), and NGC 2440, as well as relatively unexplored nebulae (M3-28, M2-48, and M3-55). In most cases, multiple molecules and transitions were used in the ratio determination, resulting in the most accurate values available to date, with 10%-40% uncertainties. The ratios found were unexpectedly low, lying in the range  $^{12}\text{C}/^{13}\text{C} \sim 1.0 \pm 0.7$ – $13.2 \pm 4.9$ , with an average value of 3.7—drastically less than found in the envelopes of C-rich AGB stars, and, in some cases, lower than the minimum value achieved in equilibrium CNO burning. Such low values are expected for the two O-rich nebulae studied (M2-9 and M2-48), because of insufficient third

dredge-up events. However, most of the PNe observed were clearly carbon-rich, as deduced from the large number of C-bearing molecules present in them. Because nucleosynthesis ceases in the PN stage, both the C/O and the  $^{12}\text{C}/^{13}\text{C}$  ratios must reflect abundances at the end of the AGB. These consistently low  $^{12}\text{C}/^{13}\text{C}$  ratios, combined with the bipolar/multipolar morphologies of all planetary nebulae observed, suggest an explosive process involving proton-capture occurred at the AGB-PN transition.

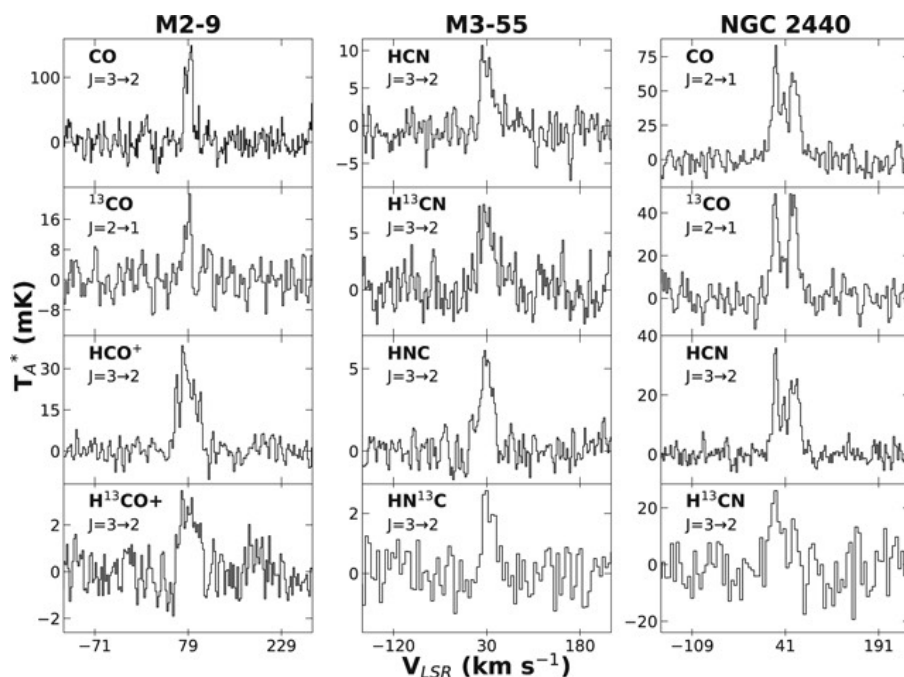


**Figure 1.** Spectra of the  $J = 3 \rightarrow 2$  transitions of  $^{12}\text{CO}$ ,  $\text{H}^{12}\text{CO}^+$ , and  $\text{H}^{13}\text{CO}^+$  and  $J = 2 \rightarrow 1$  line of  $^{13}\text{CO}$ , observed toward M2-9 (left); the  $J = 3 \rightarrow 2$  transition of  $\text{H}^{12}\text{CN}$ ,  $\text{HN}^{12}\text{C}$ ,  $\text{H}^{13}\text{CN}$ , and  $\text{HN}^{13}\text{C}$  detected toward M3-55 (middle); and the  $J = 2 \rightarrow 1$  lines of  $^{12}\text{CO}$  and  $^{13}\text{CO}$  and  $J = 3 \rightarrow 2$  lines of  $\text{H}^{12}\text{CN}$  and  $\text{H}^{13}\text{CN}$ , measured toward NGC 2440 (right). All data were obtained with the ARO SMT at 1 mm or 0.8 mm, with a spectral resolution of 2 MHz or 4 MHz ( $\text{HN}^{13}\text{C}$  and NGC 2440  $\text{H}^{13}\text{CN}$  lines). Line profiles for NGC 2440 consist of redshifted and blueshifted velocity components. In M2-9, CO spectra appear to exhibit narrower profiles than  $\text{HCO}^+$ , a likely result of Galactic contamination.

## ELT Imaging of MWC 297 from the 23 m LBTI: Complex Disk Structure and a Companion Candidate

Sallum, S.; Eisner, J. A.; Stone, J. M.; Dietrich, J.; Hinz, P.; Spalding, E.

→ [The Astronomical Journal, Volume 161, Number 1](#)

Herbig Ae/Be stars represent the early outcomes of star formation and the initial stages of planet formation at intermediate stellar masses. Understanding both of these processes requires detailed characterization of their disk structures and companion frequencies. We present new  $3.7\ \mu\text{m}$  imaging of the Herbig Be star MWC 297 from nonredundant masking observations on the phase-controlled, 23 m Large Binocular Telescope Interferometer. The images reveal complex disk structure on the scales of several au, as well as a companion candidate. We discuss physical interpretations for these features and demonstrate that the imaging results are independent of choices such as priors, regularization hyperparameters, and error-bar estimates. With an angular resolution of  $\sim 17\ \text{mas}$ , these data provide the first robust Extremely Large Telescope-resolution view of a distant young star.

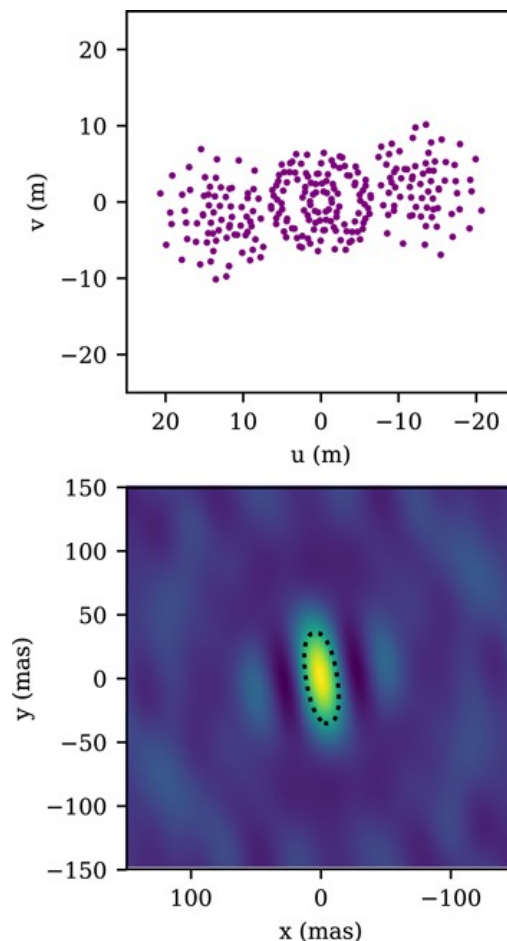


**Figure 1.** Top: scattered points show  $(u, v)$  coverage for the two MWC 297 pointings (north up, east left). Bottom: synthesized beam for the  $(u, v)$  coverage shown in the top panel (north up, east left). The dotted contour shows 50% of the peak flux.

# High-Resolution Mid-Infrared Spectroscopy of GV Tau N: Surface Accretion and Detection of Ammonia in a Young Protoplanetary Disk

Najita, Joan R.; Carr, John S.; Brittain, Sean D.; Lacy, John H.; Richter, Matthew J.; Doppmann, Greg W.

→ [Accepted for publication in The Astrophysical Journal](#)

Physical processes that redistribute or remove angular momentum from protoplanetary disks can drive mass accretion onto the star and affect the outcome of planet formation. Despite ubiquitous evidence that protoplanetary disks are engaged in accretion, the process(es) responsible remain unclear. Here we present evidence for redshifted molecular absorption in the spectrum of a Class I source that indicates rapid inflow at the disk surface. High resolution mid-infrared spectroscopy of GV Tau N reveals a rich absorption spectrum of individual lines of C<sub>2</sub>H<sub>2</sub>, HCN, NH<sub>3</sub>, and water.

From the properties of the molecular absorption, we can infer that it carries a significant accretion rate ( $\sim 1e-8$  to  $1e-7$  Msun/yr), comparable to the stellar accretion rates of active T Tauri stars. Thus we may be observing disk accretion in action. The results may provide observational evidence for

supersonic "surface accretion flows," which have been found in MHD simulations of magnetized disks. The observed spectra also represent the first detection of ammonia in the planet formation region of a protoplanetary disk. With ammonia only comparable in abundance to HCN, it cannot be a major missing reservoir of nitrogen. If, as expected, the dominant nitrogen reservoir in inner disks is instead N<sub>2</sub>, its high volatility would make it difficult to incorporate into forming planets, which may help to explain the low nitrogen content of the bulk Earth.

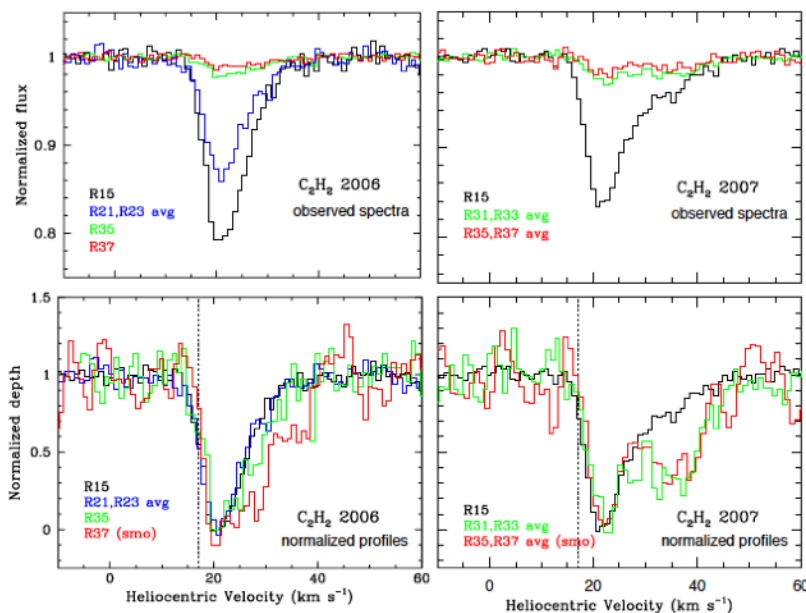


**Fig. 1.** C<sub>2</sub>H<sub>2</sub> spectra (top) and normalized line profiles (bottom) in 2006 (left) and 2007 (right). For reference, in the bottom panels, the vertical lines mark the velocity of the molecular cloud core from Hogerheijde et al. (1998). In the bottom panels, the profiles are scaled to extend from 0 at the bottom of the absorption to 1 in the continuum. The lines have an absorption core at  $v_{\text{helio}} \simeq 20 \text{ km s}^{-1}$  and a red wing extending to  $\sim 40 \text{ km s}^{-1}$ . In both epochs, the strength of the red wing relative to the core is greater in the higher energy lines (above R23) than the lower energy lines.

## An Improved HR Diagram for the Orion Trapezium Cluster

Fang, Min; Kim, Jinyoung Serena; Pascucci, Ilaria; Apai, Dániel

→ [Accepted for publication in The Astrophysical Journal](#)

In this paper, we present a study of the Trapezium cluster in Orion. We analyze flux-calibrated VLT/MUSE spectra of 361 stars to simultaneously measure the spectral types, reddening, and the optical veiling due to accretion. We find that the extinction law from Cardelli et al. (1989) with a total-to-selective extinction value of  $R_V = 5.5$  is more suitable for this cluster. For 68% of the sample the new spectral types are consistent with literature spectral types within 2 subclasses, but as expected, we derive systematically later types than the literature by one to two subclasses for the sources with significant accretion levels. Here we present an improved Hertzsprung-Russell (H-R) diagram of the Trapezium cluster, in which the contamination by optical veiling on spectral types and stellar luminosities has been properly removed. A comparison of the locations of the stars in the H-R diagram with the non-magnetic and magnetic pre-main sequence evolutionary tracks indicates an age of 1--2~Myr. The magnetic pre-main sequence evolutionary tracks can better explain the luminosities of the low-mass stars. In the H-R diagram, the cluster exhibits a large

luminosity spread ( $\sigma(\text{Log} \sim L^*/L_\odot) \sim 0.3$ ). By collecting a sample of 14 clusters/groups with different ages, we find that the luminosity spread tends to be constant ( $\sigma(\text{Log} \sim L^*/L_\odot) \sim 0.2\text{--}0.25$ ) after 2~Myr, which suggests that age spread is not the main cause of the spread. There are  $\sim 0.1$ ~dex larger luminosity spreads for the younger clusters, e.g., the Trapezium cluster, than the older clusters, which can be explained by the starspots, accretion history and circumstellar disk orientations.

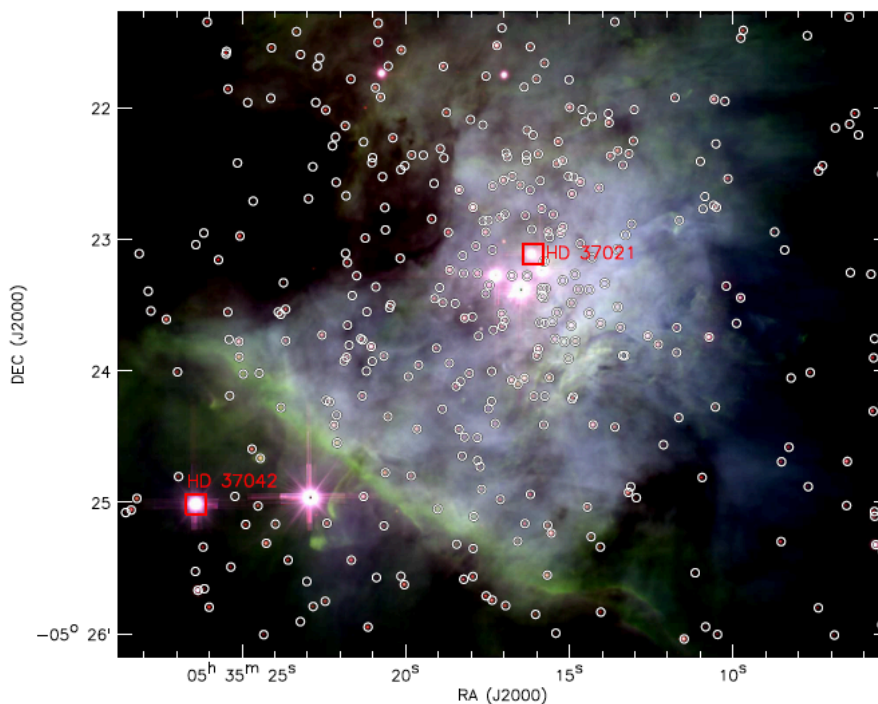


**Figure 1.** Three-color image of the Trapezium Cluster created with the MUSE data integrated over 5,000-6,000Å (blue), 6,000-7,000Å (green), and 7,500-8,500Å (red). The white open circles mark the sources for which spectra are extracted for the study in this work. Red squares show the two sources, HD 37042 and HD 37021, which were used to set and to verify the flux calibration levels.

## Proplyds in the flame nebula NGC 2024

Haworth, Thomas J.; Kim, Jinyoung S.; Winter, Andrew J.; Hines, Dean C.; Clarke, Cathie J.; Sellek, Andrew D.; Ballabio, Giulia; Stapelfeldt, Karl R.

### → [Monthly Notices of the Royal Astronomical Society, Volume 501, Issue 3](#)

A recent survey of the inner  $0.35 \times 0.35$  pc of the NGC 2024 star-forming region revealed two distinct millimetre continuum disc populations that appear to be spatially segregated by the boundary of a dense cloud. The eastern (and more embedded) population is  $\sim 0.2$ - $0.5$  Myr old, with an ALMA mm continuum disc detection rate of about 45 per cent. However, this drops to only  $\sim 15$  per cent in the 1-Myr western population. When these distinct populations were presented, it was suggested that the two main UV sources, IRS 1 (a B0.5V star in the western region) and IRS 2b (an O8V star in the eastern region, but embedded) have both been evaporating the discs in the depleted western population. In this paper, we report the firm discovery in archival HST data of four proplyds and four further candidate proplyds in NGC 2024, confirming that external photoevaporation of discs is occurring. However, the locations of these proplyds changes the picture. Only three of them are in the depleted western population and their evaporation is dominated by IRS 1, with no obvious impact from IRS 2b. The other five proplyds are in the younger eastern region and being evaporated by IRS 2b. We propose that both populations are subject to significant external photoevaporation, which happens throughout the region wherever discs are not sufficiently shielded by the interstellar medium. The external photoevaporation and severe depletion of mm grains in the  $0.2$ - $0.5$  Myr eastern part of NGC 2024 would be in competition even with very early planet formation.

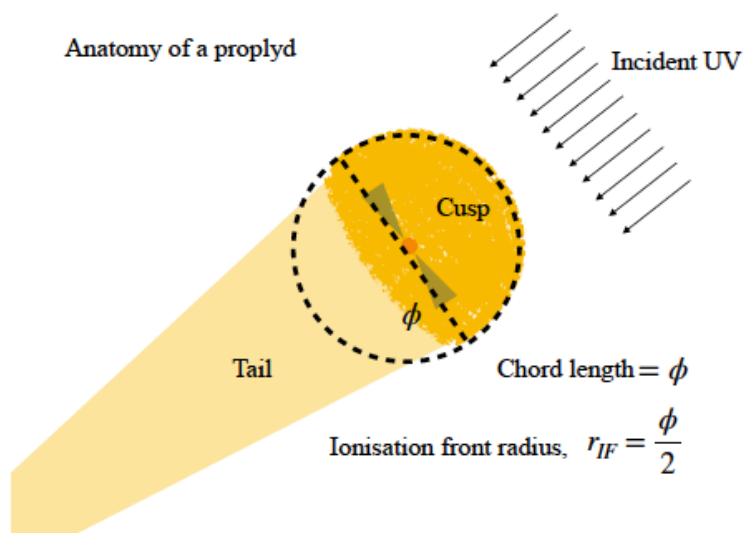


**Figure 1.** A schematic of a cometary proplyd. The disc is being irradiated by a UV field represented by the parallel arrows. This drives material from the disc into a bright cusp on the side facing the UV source and a tail on the side away from the source. When measuring the size of the proplyd (the ionisation front radius in our case) we use the radius of a circle that traces the cusp.

## The First Extensive Spectroscopic Study of Young Stars in the North America and Pelican Nebulae

Fang, Min; Hillenbrand, Lynne A.; Kim, Jinyoung Serena; Findeisen, Krzysztof; Herczeg, Gregory J.; Carpenter, John M.; Rebull, Luisa M.; Wang, Hongchi

→ [The Astrophysical Journal, Volume 904, Number 2](#)

We present a spectroscopic survey of over 3400 potential members in the North America and Pelican Nebulae (NAP) using several low-resolution ( $R \approx 1300\text{--}2000$ ) spectrographs: Palomar/Norris, WIYN/Hydra, Keck/DEep Imaging Multi-Object Spectrograph (DEIMOS), and the Multiple Mirror Telescope (MMT)/Hectospec. We identify 580 young stars as likely members of the NAP region based on criteria involving infrared excess, Li I 6708 Å absorption, X-ray emission, parallax, and proper motions. The spectral types of individual spectra are derived by fitting them with templates that are either empirical spectra of pre-main-sequence stars or model atmospheres. The templates are artificially veiled, and a best-fit combination of spectral type and veiling parameter is derived for each star. We use the spectral types with archival photometry to derive V-band extinction and stellar luminosity. From the Hertzsprung—Russell diagram, the median age of the young stars is about 1 Myr, with a luminosity dispersion of  $\sim 0.3\text{--}0.4$  dex. We investigate the photometric variability of the spectroscopic member sample using Zwicky Transient Facility data and conclude that photometric variability, while present, does not significantly contribute to the luminosity dispersion. While larger than the formal errors, the luminosity dispersion is smaller than if veiling were not taken into account in our spectral typing process. The measured ages of the

stellar kinematic groups, combined with the inferred ages for embedded stellar populations revealed by Spitzer, suggest a sequential history of star formation in the NAP region.

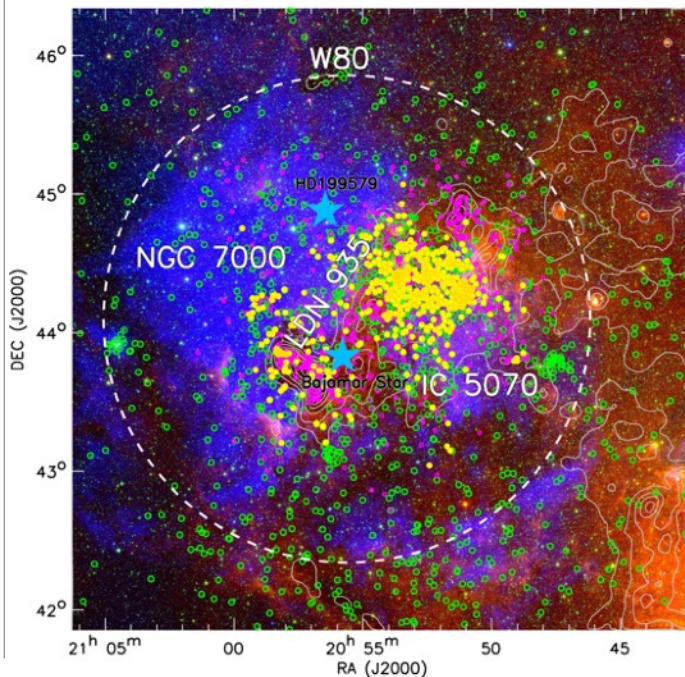


**Figure 1.** Three-color image of North America Nebula created with the DSS1 *R* band (blue), WISE W1 band (green), and WISE W3 band (red). The gray contours are the Planck 857  $\mu\text{m}$  dust emission. The white dashed circle indicates the approximate boundary of the H II region (Wendker et al. 1983). All the YSO candidates in the field are shown as open circles, magenta for those with infrared excess (Rebull et al. 2011) and green for those identified with Gaia (Kuhn et al. 2020). Our spectroscopically confirmed YSOs are shown as yellow filled circles. The blue filled star symbols mark the H II region's main ionizing source, the Balam Star, identified by Comerón & Pasquali (2005), and another member O star HD 199579 in the NAP.

## A Disk-driven Resonance as the Origin of High Inclinations of Close-in Planets

Cristobal Petrovich, Diego J. Muñoz, Kaitlin M. Kratter, and Renu Malhotra

→ [The Astrophysical Journal Letters, Volume 902, Number 1](#)

The recent characterization of transiting close-in planets has revealed an intriguing population of sub-Neptunes with highly tilted and even polar orbits relative to their host star's equator. Any viable theory for the origin of these close-in, polar planets must explain (1) the observed stellar obliquities, (2) the substantial eccentricities, and (3) the existence of Jovian companions with large mutual inclinations. In this work, we propose a theoretical model that satisfies these requirements without invoking tidal dissipation or large primordial inclinations. Instead, tilting is facilitated by the protoplanetary disk dispersal during the late stage of planet formation, initiating a process of resonance sweeping and parametric instability. This mechanism consists of two steps. First, a nodal secular resonance excites the inclination to large values; then, once the inclination reaches a critical value, a linear eccentric instability is triggered, which detunes the resonance and ends inclination growth. The critical inclination is pushed to high values by general relativistic precession, making polar orbits an inherently post-Newtonian outcome. Our model predicts that polar, close-in sub-Neptunes coexist with cold Jupiters in low stellar obliquity orbits.

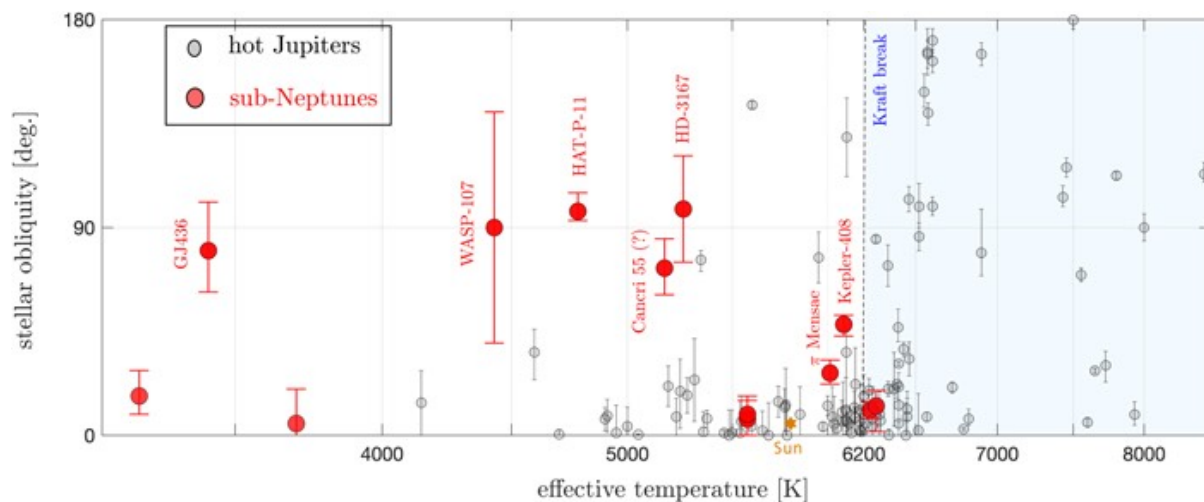


**Figure 1.** Measured stellar obliquity for close-in planets ( $a \lesssim 0.1$  au) as a function of the host star's effective temperature. The gray circles show the sample of hot Jupiters ( $M_p > 0.3M_J$  and  $P < 10$  days) with reliable obliquity measurements ( $1-\sigma$  errors  $< 20^\circ$ ). The larger red circles show the sample of planets with either sizes or masses comparable to or smaller than that of Neptune, specifically  $R_p < 6R_\oplus$  and/or  $M_p < 30M_\oplus$ . The data is taken from the TEPcat Catalog as of 2020 August (Southworth 2011, <http://www.astro.keele.ac.uk/jkt/tepcat>) with most values corresponding to projected stellar obliquities, though a small fraction are non-projected values. When both are available, we use the latter.

## Observational Completion Limit of Minor Planets from the Asteroid Belt to Jupiter Trojans

Nathanial P. Hendler and Renu Malhotra

→ [The Planetary Science Journal, Volume 1, Number 3](#)

With the growing numbers of asteroids being discovered, identifying an observationally complete sample is essential for statistical analyses and for informing theoretical models of the dynamical evolution of the solar system. We present an easily implemented method of estimating the empirical observational completeness in absolute magnitude,  $H_{\text{lim}}$ , as a function of semimajor axis. Our method requires fewer assumptions and decisions to be made in its application, making results more transportable and reproducible among studies that implement it, as well as scalable to much larger data sets of asteroids expected in the next decade with the Vera C. Rubin Observatory's Legacy Survey of Space and Time. Using the values of  $H_{\text{lim}}(a)$  determined at high resolution in semimajor axis,  $a$ , we demonstrate that the observationally complete sample size of the main belt asteroids is larger by more than a factor of 2 compared with using a conservative single value of  $H_{\text{lim}}$ , an approach often adopted in previous studies. Additionally, by fitting a simple, physically motivated model of  $H_{\text{lim}}(a)$  to  $\sim 7 \times 10^5$  objects in the Minor Planet Database, our model reveals statistically significant deviations between the main belt and the asteroid populations beyond the main belt (Hungarias, Hildas, and Trojans), suggesting potential demographic differences, such as in their size, eccentricity, or inclination distributions.

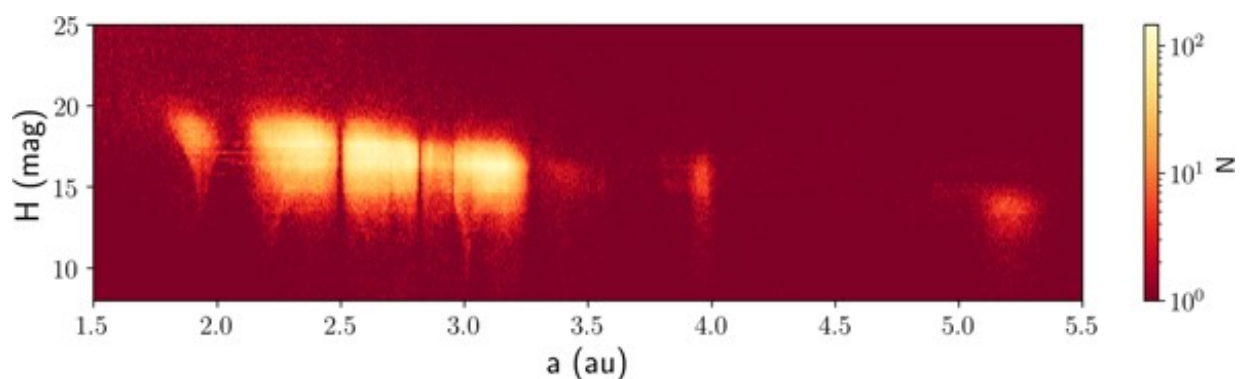


**Figure 1.** Heatmap of observed  $H$  magnitude for minor planets with a semimajor axis between 1.5 and 5.5 au. This range of semimajor axes includes the Hungarias, main belt asteroids, Hildas, and Trojans. The regions of greatest population density are shown in yellow. The completion limit as a function of semimajor axis,  $a$ , is evident by eye as a downward sloping trend in the upper envelope of the highest density regions.